

Entanglement-enhanced Optomechanical Sensing

Yi Xia^{1,2}, Aman R. Agrawal¹, Christian M. Pluchar¹, Quntao Zhuang^{3,1}, Dalziel J. Wilson¹, Zheshen Zhang^{2,3,1}

1. *James C. Wyant College of Optical Sciences, University of Arizona, Tucson, Arizona 85721, USA*

2. *Department of Materials Science and Engineering, University of Arizona, Tucson, Arizona 85721, USA*

3. *Department of Electrical and Computer Engineering, University of Arizona, Tucson, Arizona 85721, USA*

zsz@arizona.edu

Abstract: We experimentally demonstrate entanglement-enhanced optomechanical sensing in which entangled optical probes jointly read out the displacements of two mechanical membranes, enabling enhanced force sensitivities and enlarged measurement bandwidths.

© 2022 The Author(s)

Optomechanical sensors have been used to make ultrasensitive measurements of force, acceleration, and magnetic fields. To overcome the measurement imprecision arising from the optical shot noise, squeezed light has been harnessed to enhance the performance of a single optomechanical sensor [1]. Joint measurements taken by multiple optomechanical sensors can further improve the measurement sensitivity and enable distributed sensing capabilities. A pathway toward quantum enhancements in this multi-sensor regime, however, has not been explored. In this work, we theoretically show and experimentally demonstrate how entangled light can be leveraged to enhance the performance of multiple optomechanical sensors in detecting force signals. In the experiment, entangled optical probes jointly read out the displacements of two mechanical membranes and achieve a measurement sensitivity 2 dB below the shot-noise limit set by classical probes.

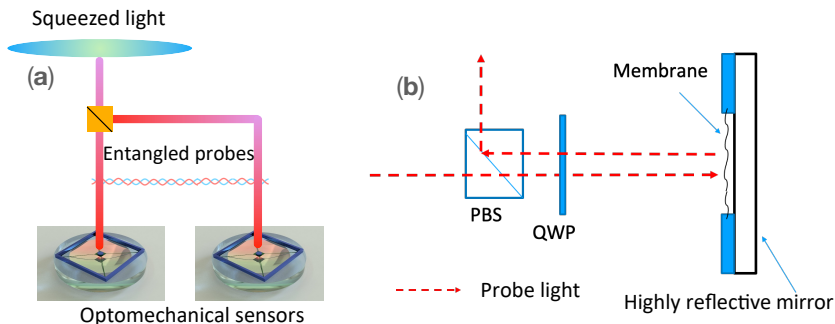


Fig. 1. (a) Experiment setup. (b) Membrane-based optomechanical sensor. QWP: quarter-wave plate; PBS: polarizing beam splitter.

Our experimental setup is shown in Fig. 1 (a). Entangled probes are generated by splitting phase-squeezed light into two arms, in the same vein as the recent entangled sensor network experiments [2, 3]. Each arm carries 60 μW of optical power and probes an optomechanical sensor formed by placing a $100 \times 100 \mu\text{m}^2$ Si_3N_4 membrane with a reflectively $R \approx 11.5\%$ atop a high reflectively ($R > 99.9\%$) mirror, forming a Finesse ~ 3 optical cavity, as illustrated in Fig. 1 (b). Each membrane supports a high-Q drum mode encoding the signal, with resonance frequencies $\Omega_1/2\pi = 5.948 \times 10^6$ Hz and $\Omega_2/2\pi = 5.9494 \times 10^6$ Hz with damping rates $\Gamma_1/2\pi = 247$ Hz and $\Gamma_2/2\pi = 193$ Hz, respectively.

In Fig. 2, we present displacement measurements of two membranes. Specifically, we measure the phase quadrature $\hat{Y}_{\text{out}}^i(\omega) = \hat{Y}_{\text{in}}^i(\omega) + \alpha_i \beta_i \chi_i(\omega) \hat{F}_{\text{th}}^i$ of the output probe light using balanced homodyne detectors. Here, $i = 1, 2$ is the index of the sensors, \hat{Y}_{in} is the phase quadratures of the input probes, α_i , β_i , and χ_i are, respectively, the probe amplitude, the transduction efficiency, and the mechanical susceptibility, and \hat{F}_{th}^i is the thermal force. The measured noise PSD for sensor 1 (blue) and 2 (magenta) are plotted in Fig. 2 (a). As a comparison, we plot the measured noise PSD using classical light with the same probe power in Fig. 2 (b). In both measurements, the shot noise is normalized to unity. Thermal noise dominates in the vicinity of resonant frequencies, yielding noise peaks of equal magnitude for the entangled and classical probes. In contrast, shot noise dominates over the off-resonant frequencies when classical probes are employed. The introduction of entangled probes reduces the off-resonant noise floor by 1 dB, as shown in Fig. 2 (a). We next derive the noise PSD of a joint measurement of the sum of

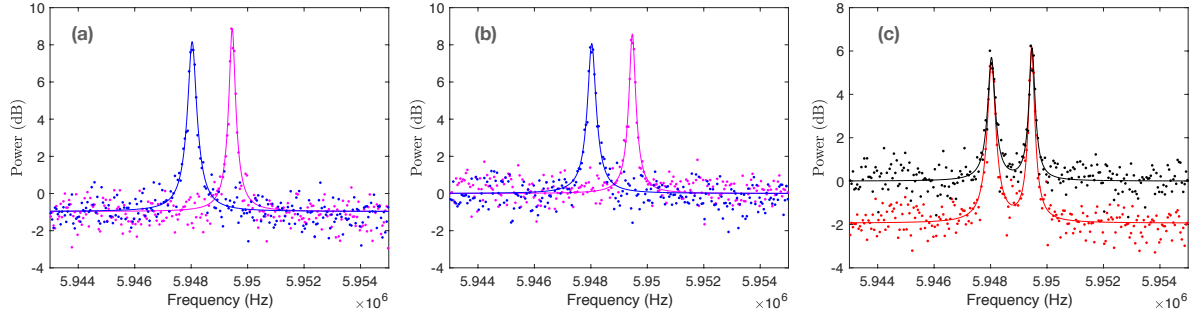


Fig. 2. Individual-measurement noise PSDs of membrane 1 (blue) and membrane 2 (magenta) using (a) entangled probes and (b) classical probes. (c) Joint-measurement noise PSDs using classical (black) or entangled (red) probes. In all figures, dots: experiment; solid lines: theory. Probe power: 60 μ W.

the displacements taken by both sensors. The joint PSD depicted in Fig. 2 (c) shows a 2 dB disparity between the noise PSDs at off-resonant frequencies when entangled probes are on (red) and off (black), while the power of the two thermal peaks are preserved near the resonances. This is because thermal noise is uncorrelated so they add up incoherently whereas entanglement between the probes leads to the cancellation of the measurement noise at off-resonant frequencies.

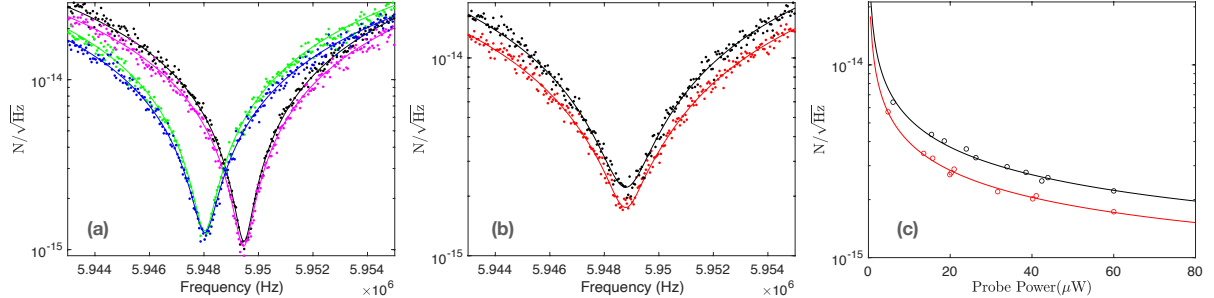


Fig. 3. Force-sensitivity data. (a) Force sensitivity at individual sensors. Entangled probes: blue, magenta; classical probes: green, black (b) Joint force sensitivity of both sensors. Entangled probes: red; classical probes: black. (c) Joint sensitivity at different probe power. Entangled probes: red; classical probes: black. In all figures, dots: experimental data; solid lines: theory.

The optomechanical sensors can be utilized for force measurements. The sensitivities of force measurements are derived by rescaling the phase quadratures of probes: $\hat{Y}_{\text{out}}^i(\omega)/(\alpha_i \beta_i \chi_i(\omega))$. Shown in Fig. 3 (a) for both the entangled and classical probes, the force sensitivity is limited by the thermal forces $\sqrt{S_{F_{\text{th}}^i} F_{\text{th}}^i} = \sqrt{2\Gamma_i m_{\text{eff}} k_B T} \sim 10^{-15} \text{ N}/\sqrt{\text{Hz}}$, where Γ_i is the oscillator damping rate, m_{eff} is the effective mass, k_B is the Boltzmann constant, and T is temperature. At each sensor, the measurement bandwidth with entangled probes (magenta, blue) is only slightly improved over that associated with classical probes (green, black) due to the 1 dB shot noise reduction enabled by the residue squeezing. By contrast, entangled probes (red) enhance the force sensitivity achieved by classical probes (black) by 22% in a joint measurement of the average force, whose minimal sensitivity resides at a shot-noise-dominant region in between the two resonant frequencies. The joint force sensitivities vs the probe power are plotted in Fig. 3 (c), showing again an entanglement-enabled sensitivity advantage.

In conclusion, we have experimentally demonstrated entanglement-enhanced joint measurements taken by two optomechanical sensors. Our work opens a new avenue for ultraprecise measurements with an array of quantum-enhanced sensors for applications ranging from inertial navigation to acoustic imaging and to searches for new physics.

References

1. B. Li, *et al.*, “Quantum enhanced optomechanical magnetometry,” *Optica* **5**, 7 (2018).
2. Y. Xia, W. Li, W. Clark, D. Hart, Q. Zhuang, and Z. Zhang, “Demonstration of a reconfigurable entangled radio-frequency photonic sensor network,” *Phys. Rev. Lett.* **124**, 150502 (2020).
3. X. Guo *et al.*, Distributed quantum sensing in a continuous-variable entangled network, *Nat. Phys.* **16**, 281 (2020).